Unveiling correlation between α_2 relaxation and yielding behavior in metallic glasses

Zhen-Ya Zhou,[1] Qing Chen,[1] Yang Sun,[2,*] and Hai-Bin Yu[1,†]

[1]*Wuhan National High Magnetic Field Center and School of Physics, Huazhong University of Science and Technology, Wuhan 430074, China*

[2]*Department of Applied Physics and Applied Mathematics, Columbia University, New York, New York 10027, USA*

(Received 8 November 2020; accepted 19 March 2021; published 29 March 2021)

Relaxation processes usually influence the mechanical properties of glassy materials. Recently, a so-called α_2 relaxation has been identified in metallic glasses, caused by the mobility decoupling between different constituting atoms. It locates between the primary (α) relaxation and the secondary (β) relaxation and behaves as an additional α relaxation. In this paper, we show that α_2 relaxation influences the yielding behaviors of a model $Al_{90}Sm_{10}$ metallic glass. In particular, the transition from the stress overshoot to nonovershoot yielding and α_2 relaxation follow the same time-temperature relation and microscopic origin. Our results suggest that α_2 relaxation provides an additional way to control the mechanical properties of metallic glasses.

DOI: 10.1103/PhysRevB.103.094117

I. INTRODUCTION

Glassy materials [1–11] feature several types of relaxations [12–18] that influence the mechanical properties of the materials. We showcase the relationship between relaxations and mechanical properties in the schematic shown in Fig. 1. Specifically, the primary relaxation mode, α relaxation, is related to viscous flow and glass transition [19]. At temperatures above α relaxation the material can flow with a low shear modulus (i.e., a supercooled liquid), while at low temperatures the material is a solid (i.e., the glass). In the intermediate temperature regime, the secondary β relaxation [12,20–31] is correlated with the shear transformation zones (STZs) [32–36] and the ductility of the metallic glasses (MGs) and polymers [37–40]. At even lower temperatures (below room temperature), researchers observed an unusually fast β' relaxation process in rare-earth-based metallic glasses [41,42], which occurs at a temperature far below the glass transition point with a low activation energy. It was suggested that this fast secondary relaxation affects the low-temperature plasticity [43].

Furthermore, research found that the boson peak [44–57] is related to the distribution and activation of flow units, thus indicating that the boson peak could correlate with the mechanical properties of MGs [45,51]. Luo *et al.* [58] reported that nonequilibrium α relaxation would split into two processes in a deep glassy state, which causes an early decay in stress-relaxation experiments.

We note that while the mechanical properties and the relaxation dynamics are usually studied by different stress/strain levels, the correlations between them might imply the existence of underlying structure-properties connections, which is a long-standing aim of the studies of glassy materials. Unlike crystalline materials, such a link is difficult to establish solely from static structures. Therefore the studies of relaxation dynamics offer an alternative approach to this issue.

More recently, Sun *et al.* [59] revealed that there is an anomalous relaxation process (α_2) accompanying α relaxation in Al-Sm metallic glass, which is found to correlate with the decoupling of the faster motions of Al and slower Sm atoms. This α_2 relaxation locates at the temperature regime in between α relaxation and β relaxation, and shows a similarity with α relaxation. Specifically, the peak intensity decreases with temperature, following a similar trend as α relaxation, but not β relaxation. Although it is newly identified, some earlier data indeed show signatures of its presence in several metallic glasses [60]. Currently it is still unclear whether the newly discovered α_2 relaxation is related to any mechanical properties.

In this paper, we provide computational evidence to demonstrate a close link between the α_2 relaxation and yielding behaviors. We show that the characteristic times of α_2 relaxation and the stress-overshoot to nonovershoot-yielding transition (SNT) are nearly identical. Furthermore, during the SNT, we find the atomic motion decoupling phenomenon is consistent with the one in α_2 relaxation. Based on the combined findings, we attempt to understand the fundamental mechanism of SNT and α_2 relaxation in metallic glasses by correlating the α_2 relaxation and SNT with a common characteristic time and the same microscopic origin.

II. COMPUTATIONAL DETAILS

Molecular dynamics (MD) simulations were employed to study the tensile deformation behavior of $Al_{90}Sm_{10}$ metallic glass. The $Al_{90}Sm_{10}$ glass model, containing 32 000 atoms, was obtained by continuous cooling with a cooling rate of 10^8 K/s in the *NPT* ensemble (that is, a constant number of atoms, pressure, and temperature). At different temperatures and strain rates, the tensile strain was applied as shown in the

*ys3339@columbia.edu
†habinyu@hust.edu.cn

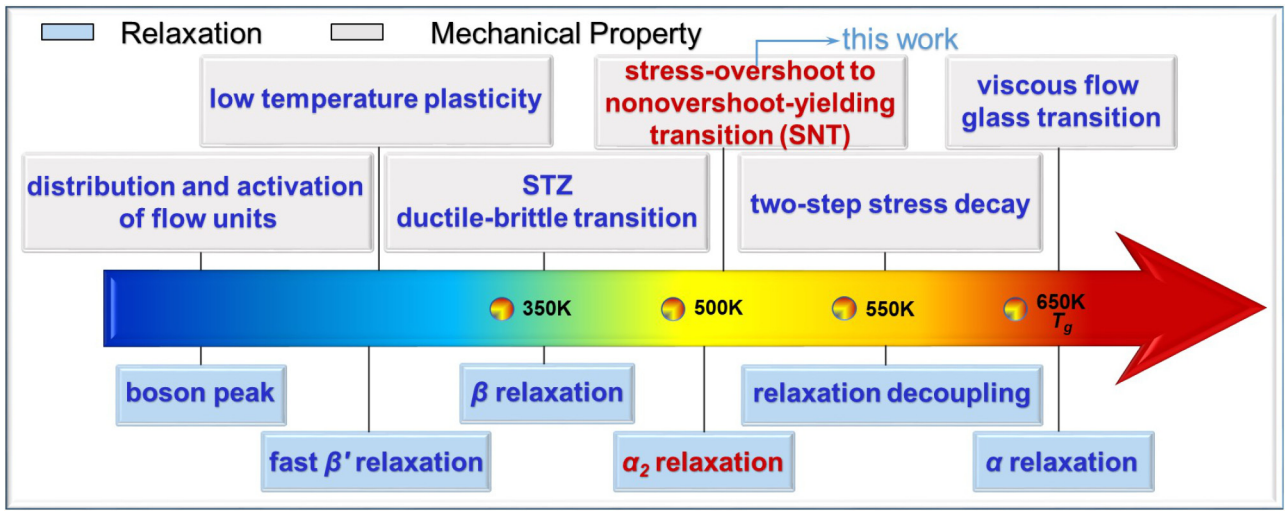

FIG. 1. The correlation between relaxations and mechanical properties. The characteristic temperatures are based on $Al_{90}Sm_{10}$ metallic glass as an example. The characteristic temperature of a fast β' relaxation process is typically lower than room temperature in rare-earth-based metallic glasses (∼200 K). The boson peak usually occurs at an extremely low temperature (∼10 K).

inset of Fig. 2(a). Specifically, at a temperature T, a tensile strain $\varepsilon(t) = \dot{\varepsilon} \cdot t$, with a constant strain rate $\dot{\varepsilon}$ was applied along the x direction. The resulting stress σ_x was recorded for the analysis. All MD simulations were performed with the LAMMPS package [61–64] using the Finnis-Sinclair potential [65]. Periodic boundary conditions were applied in all three directions.

III. RESULTS

A. The yielding behavior and relaxation map of $Al_{90}Sm_{10}$ model MGs

Figure 2 shows the stress-strain curves of $Al_{90}Sm_{10}$ MGs from MD simulations. The upper and lower panels show the change of the stress-strain curve with different temperatures

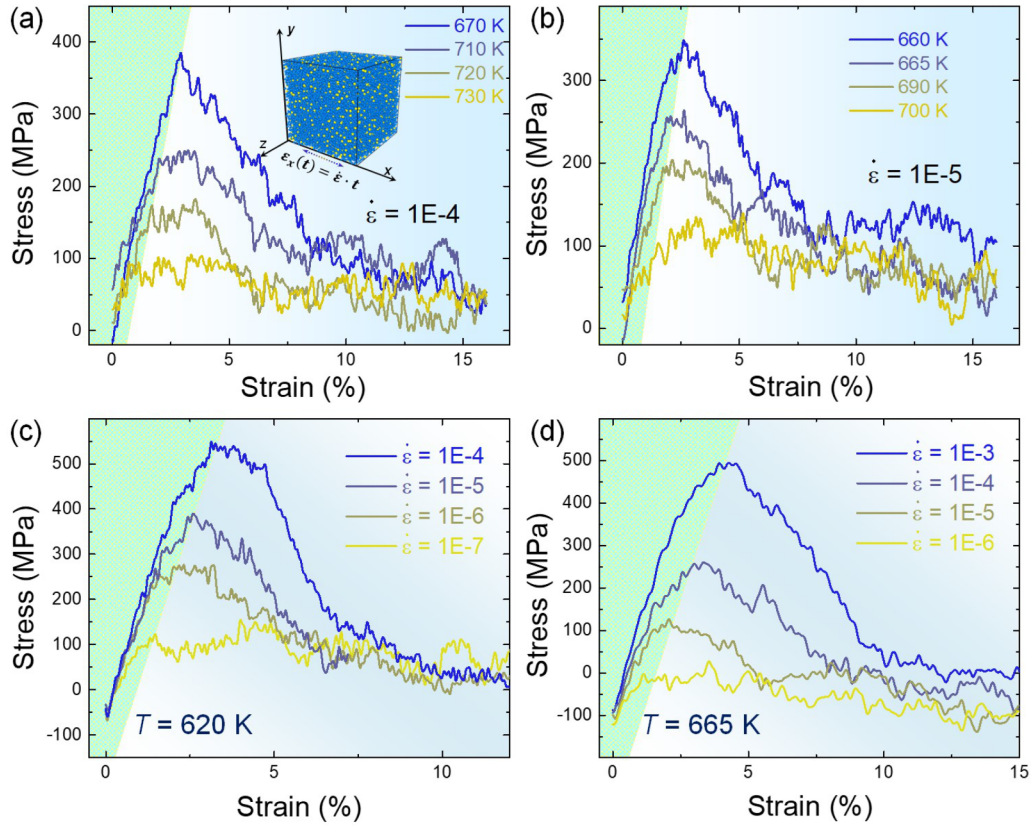

FIG. 2. Computational stress-strain curves at different temperatures and strain rates in $Al_{90}Sm_{10}$ model MGs. The green shallow region represents the elastic range in deformation.

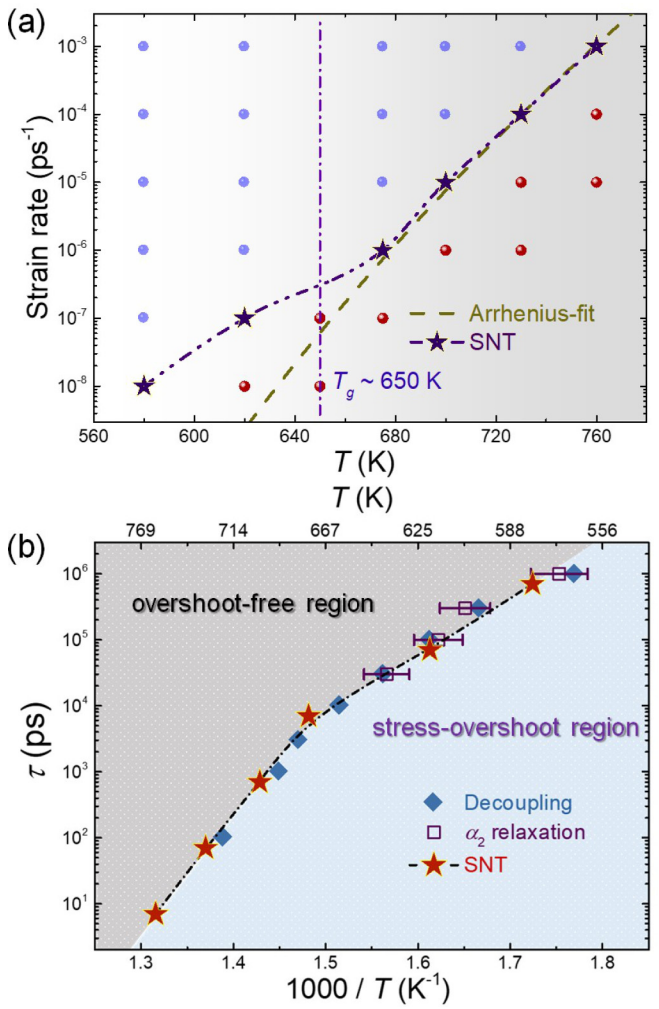

FIG. 3. The deformation and relaxation map of $Al_{90}Sm_{10}$ model MGs. (a) The deformation mode map summarizing the tension simulations at different temperatures and strain rates in $Al_{90}Sm_{10}$ model MGs. The blue balls denote the systems with a significant yield overshoot while the red balls are direct plastic flow systems, and the SNT is represented by a pentagram with the dotted line to guide the eyes. T_g of $Al_{90}Sm_{10}$ model MG is about 650 K with the current cooling rate. (b) The correlation between α_2 relaxation and SNT of $Al_{90}Sm_{10}$ model MGs.

and strain rates, respectively. All the stress-strain curves in this paper are obtained with the same protocol. As a typical example, Fig. 2(a) shows the evolution of stress measured during tensile deformation with a strain rate of $\dot{\varepsilon} = 10^{-4}$/ps at different temperatures. At a relatively low temperature ($T = 670$ K), the model MG reaches the plastic flow state after an initial yield overshoot. The yielding point of this case is $\varepsilon = 2.9\%$. With a higher temperature, the yield overshoot continuously decreases and disappears at 730 K. The yielding point also gradually decreases from 2.9% to 1.1%. A qualitatively similar trend can be seen in Fig. 2(b), where the strain rate is ten times slower than the one in Fig. 2(a). In Figs. 2(c) and 2(d), the temperature is fixed while the strain rate is varied in a range of three orders of magnitudes. By comparing the results under different conditions in Fig. 2, one can find that the effect of decreasing strain rate at a constant temperature is qualitatively similar to the effect of increasing temperature under a constant strain rate. It shows that under different conditions, the stress-strain curves always exhibit a transition accompanying the change of yield overshoot. Here, the critical point where the yielding overshoot disappears is selected to characterize the SNT. The current data demonstrate the deformation of $Al_{90}Sm_{10}$ MG is very sensitive to the loading rate and temperature. It is worth noting that in some cases where the temperature is higher than T_g, the stress-strain curve shows a clear stress-overshoot yielding. This is mainly due to the fast loading rate, because the glass transition is rate dependent, and at the timescale of the yielding measurement it may be even higher. This observation is consistent with some previous experiments [35,66].

By sampling a wide range of temperatures and strain rates, we map different deformation modes in Fig. 3(a). Under the condition of lower temperature or faster strain rate, the stress-strain curve usually shows a significant yield overshoot. As the temperature increases or the strain rate slows down, the yield overshoot gradually disappears. Once passing the SNT, the system directly enters the plastic flow without a yield overshoot. The temperature dependence of the SNT point shows the Arrhenius relationship at higher temperatures. However, it quickly deviates from the Arrhenius curve when the temperature becomes lower than the glass transition temperature.

In order to understand the correlation between SNT and relaxation more comprehensively, we further analyze the characteristic temperature of SNT. In polymer glasses, there is an empirical relation between the strain rates $\dot{\varepsilon}$ and equivalent frequency f, $f = A\dot{\varepsilon}$, with constant $A \approx 143$. Using this relation, we translate the strain rates in tensile tests into effective frequencies. In this way, we are able to represent the SNT in a temperature-time relationship as shown in Fig. 3(b). By summarizing the α_2 relaxation and atom decoupling process in a relaxation map, we find that the α_2 relaxation and the decoupling between Sm and Al atoms follow the same temperature-time relation as SNT, suggesting an intrinsic correlation among them. More importantly, the data reveal a nearly one-to-one correspondence between α_2 relaxation and SNT that extends over a broad temperature range.

B. The microscopic origin of SNT of $Al_{90}Sm_{10}$ model MGs

To grasp the microscopic origin of SNT and α_2 relaxation, we analyze the probabilities $p(u)$ of atomic displacements u for Al and Sm atoms during tensile deformation, respectively. Here, the atomic displacement u is calculated from the initial state to the time of reaching 10% strain. As shown in Fig. 4(a), at a strain rate $\dot{\varepsilon} = 10^{-4}$/ps higher than the critical point of SNT (about 10^{-7}/ps) with a constant temperature ($T = 620$ K), the peaks of $p(u)$ for Al and Sm deviate from each other, while at the strain rate $\dot{\varepsilon} = 10^{-7}$/ps reaching the SNT, the $p(u)$ peaks of Al and Sm well overlap. This comparison implies that decoupling of the motions of Al and Sm atoms occurs when the strain rate crosses the SNT.

Figure 4(b) plots the most probable displacement, i.e., the peak position u_p of $p(u)$ as a function of temperature

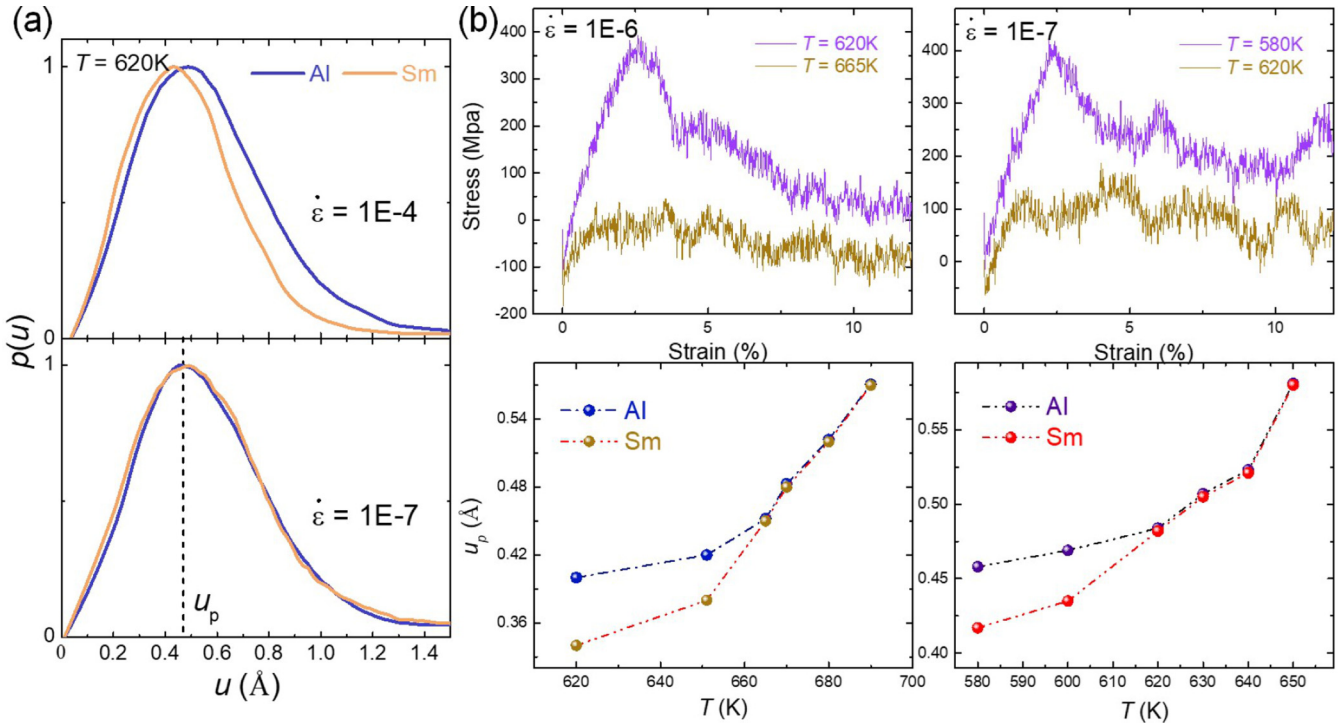

FIG. 4. Atomic motion decoupling in tensile deformation at different temperatures and strain rates. (a) The probability of Al and Sm displacement with a strain rate at $\dot{\varepsilon} = 10^{-4}$/ps and $\dot{\varepsilon} = 10^{-7}$/ps, respectively. The dashed line indicates the peak position u_p. (b) u_p of Al and Sm atoms and strain-stress curves at different temperatures and strain rates, respectively.

at two different strain rates to further quantify this behavior. When the temperature increases from the lower regime, the u_p of Al and Sm atoms first increase separately until reaching a transition point where the two curves merge into one. When comparing u_p with the strain-stress curve in Fig. 4(b), we find that the transition point coincides with the critical point of SNT over all the studied strain rates and temperatures. Therefore, the SNT correlates well with the dynamical transition from coupling to decoupling motions of Al and Sm atoms during tensile deformation. In other words, the fast and slow motions freeze asynchronously at relatively low temperatures or fast strain rates.

The above results draw attention to a more general question: What are the specific modes of the atomic movement decoupling and coupling in the process of tensile deformation? In Fig. 5, we visually analyze the displacement of atoms at 620 K in various strain rates with OVITO [67] to understand the specific decoupling and coupling mode. As shown in Fig. 5(e), the displacement of most atoms is between 0 and 1.5 Å. Therefore, we select the atoms with displacement in this range in a slice of the simulation box for clarity. At a relatively fast strain rate ($\dot{\varepsilon} = 10^{-4}$/ps), Al and Sm atoms move randomly in all directions. When the strain rate slows down and reaches SNT, the movement patterns of Al and Sm atoms become more collective. A large number of Al and Sm atoms move together in the same direction and form clusters. In a few cases, Al and Sm atoms form a stringlike motion. In Fig. 5(f), we zoom in these areas from Fig. 5(d) in order to visualize the strongly coupled displacement.

IV. DISCUSSION AND CONCLUSION

Our results suggest that with a slower tensile deformation, the atomic motions change from disordered decoupling to the collective atomic flow. The coupled flow may release the stress, which makes the overshoot deformation disappear. Meanwhile, as an amorphous yield can be viewed as a transition from localized to extended plastic activity, these coupled flow areas can be regarded as specific manifestations of extended plastic activities. As a typical glass system, $Al_{90}Sm_{10}$ MG exhibits multiple relaxation modes and its solute and solvent elements exhibit very different dynamical behaviors [59]. The identified SNT in this paper shows the same microscopic origin with a recently identified α_2 relaxation and both of them exhibit a consistent characteristic time. It indicates that the SNT can be regarded as the macromanifestation of α_2 relaxation, similar to the connection between a glass transition and α relaxation.

In summary, by conducting MD simulations, we have revealed the SNT during tensile deformation and clarified its microscopic origins. By analyzing the atomic motion in tensile deformation, we show that the emergence of SNT is due to the mobility decoupling of the solute and solvent atoms. Similar microscopic origins lead to a consistent time-temperature relationship between SNT and α_2 relaxation. With the above interpretations, one would expect to associate SNT with α_2 relaxation, or even more broadly link mechanical behavior with relaxation. It then suggests that efforts aimed at a quantitative theory to analyze the structure origin of mechanical behavior and relaxation would be desirable. The results presented above thus open different challenges and opportunities

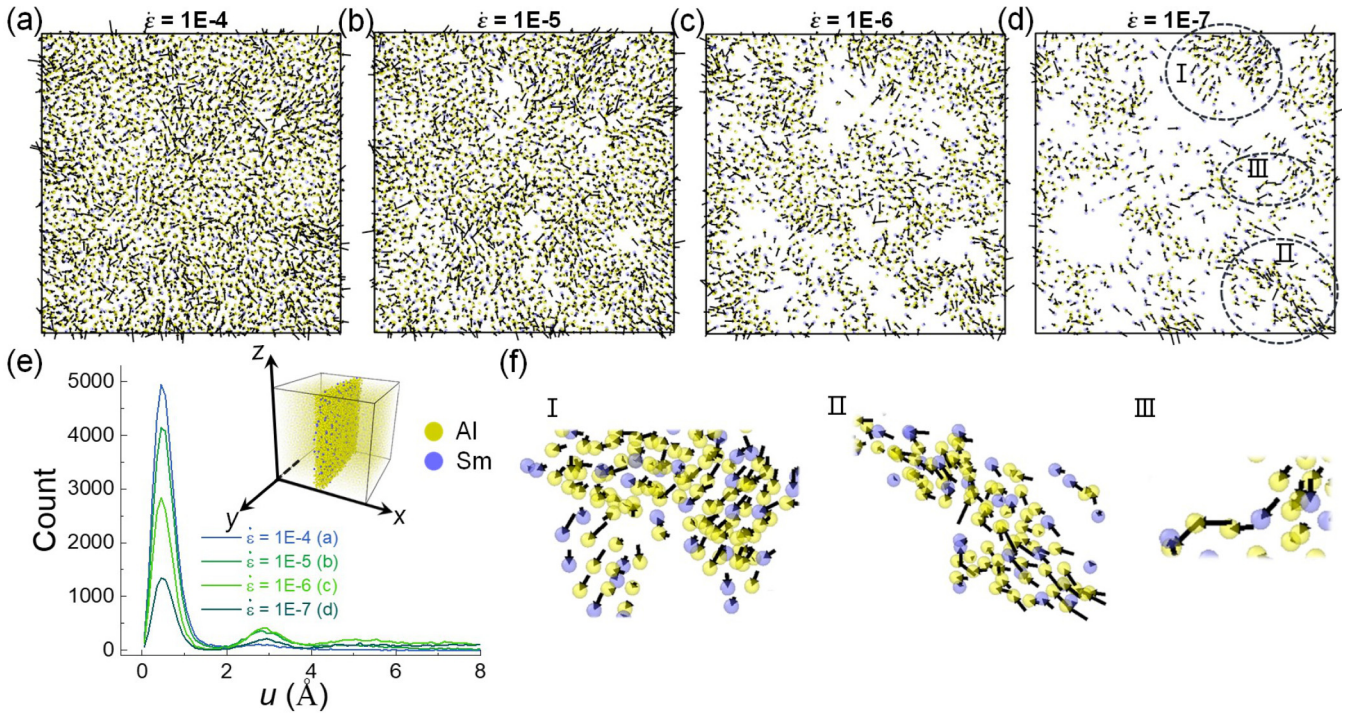

FIG. 5. Decoupling and coupling mechanism diagram at 620 K. (a)–(d) A snapshot extracted from simulations at several strain rates after slicing. (e) Statistical map of atomic displacement at different strain rates. The illustration shows the selection range of the slice. (f) Enlarged view of the dotted area in (d). All maps select the time when each strain reaches 10%.

for furthering our understanding of mechanical behavior and glass relaxations.

ACKNOWLEDGMENTS

The computational work was carried out using the Tianhe-1A of the National Supercomputer Center in Tianjin, China, the Tianhe-2 of the National Supercomputer Center in Guangzhou, China and supported by the public computing service platform provided by the Network and Computing Center of HUST. We are thankful for support from the National Science Foundation of China (NSFC 52071147 and 51601064) and the National Thousand Young Talents Program of China. Y.S. was supported by NSF Award No. EAR-1918126.

[1] A. L. Greer, Science **267**, 1947 (1995).
[2] W. K. Klement, R. H. Willens, and P. Duwez, Nature (London) **187**, 869 (1960).
[3] W. L. Johnson, MRS Bull. **24**, 42 (1999).
[4] W. Wang, C. Dong, and C. Shek, Mater. Sci. Eng., R **44**, 45 (2004).
[5] H. W. Sheng, W. K. Luo, F. M. Alamgir, J. M. Bai, and E. Ma, Nature (London) **439**, 419 (2006).
[6] A. Hirata, L. J. Kang, T. Fujita, B. Klumov, K. Matsue, M. Kotani, A. R. Yavari, and M. W. Chen, Science **341**, 376 (2013).
[7] E. D. Cubuk, R. J. S. Ivancic, S. S. Schoenholz, D. J. Strickland, A. Basu, Z. S. Davidson, J. Fontaine, J. L. Hor, Y. R. Huang, Y. Jiang, N. C. Keim, K. D. Koshigan, J. A. Lefever, T. Liu, X. G. Ma, D. J. Magagnosc, E. Morrow, C. P. Ortiz, J. M. Rieser, A. Shavit *et al.*, Science **358**, 1033 (2017).
[8] V. Bapst, T. Keck, A. Grabska-Barwińska, C. Donner, E. D. Cubuk, S. S. Schoenholz, A. Obika, A. W. R. Nelson, T. Back, D. Hassabis, and P. Kohli, Nat. Phys. **16**, 448 (2020).
[9] J. Pan, Q. Chen, L. Liu, and Y. Li, Acta Mater. **59**, 5146 (2011).
[10] H. Tong and H. Tanaka, Phys. Rev. Lett. **124**, 225501 (2020).
[11] H. Tanaka, H. Tong, R. Shi, and J. Russo, Nat. Rev. Phys. **1**, 333 (2019).
[12] G. P. Johari, J. Chem. Phys. **58**, 1766 (1973).
[13] C. A. Angell, K. L. Ngai, G. B. McKenna, P. F. McMillan, and S. W. Martin, J. Appl. Phys. **88**, 3113 (2000).
[14] P. Lunkenheimer, U. Schneider, R. Brand, and A. Loid, Contemp. Phys. **41**, 15 (2000).
[15] J. C. Dyre, Rev. Mod. Phys. **78**, 953 (2006).
[16] K. L. Ngai, *Relaxation and Diffusion in Complex Systems* (Springer, New York, 2011).
[17] S. Capaccioli, M. Paluch, D. Prevosto, L. Wang, and K. L. Ngai, J. Phys. Chem. Lett. **3**, 735 (2012).
[18] Q. Yang, S. X. Peng, Z. Wang, and H. B. Yu, Natl. Sci. Rev. **7**, 1896 (2020).
[19] S. Torquato, Nature (London) **405**, 521 (2000).
[20] L. Hu and Y. Yue, J. Phys. Chem. C **113**, 15001 (2009).
[21] D. D. Liang, X. D. Wang, Y. Ma, K. Ge, Q. P. Cao, and J. Z. Jiang, J. Alloy Compd. **577**, 257 (2013).
[22] J. C. Qiao and J. M. Pelletier, J. Appl. Phys. **112**, 083528 (2012).

[23] P. Rösner, K. Samwer, and P. Lunkenheimer, Europhys. Lett. **68**, 226 (2004).
[24] Z. Wang, H. B. Yu, P. Wen, H. Y. Bai, and W. H. Wang, J. Phys.: Condens. Matter **23**, 142202 (2011).
[25] Z. F. Zhao, P. Wen, C. H. Shek, and W. H. Wang, Phys. Rev. B **75**, 174201 (2007).
[26] G. P. Johari and M. Goldstein, J. Chem. Phys. **53**, 2372 (1970).
[27] H. B. Yu, R. Richert, and K. Samwer, Sci. Adv. **3**, e1701577 (2017).
[28] H. B. Yu, W. H. Wang, H. Y. Bai, and K. Samwer, Natl. Sci. Rev. **1**, 429 (2014).
[29] H. B. Yu, W. H. Wang, and K. Samwer, Mater. Today **16**, 183 (2013).
[30] Y. B. Yang, Q. Yang, D. Wei, L. H. Dai, H. B. Yu, and Y. J. Wang, Phys. Rev. B **102**, 174103 (2020).
[31] Z. Y. Zhou, H. L. Peng, and H. B. Yu, J. Chem. Phys. **150**, 204507 (2019).
[32] A. S. Argon, Acta Metall. **27**, 47 (1979).
[33] M. L. Falk and J. S. Langer, Phys. Rev. E **57**, 7192 (1998).
[34] C. Maloney and A. Lemaître, Phys. Rev. Lett. **93**, 016001 (2004).
[35] C. A. Schuh, T. C. Hufnagel, and U. Ramamurty, Acta Mater. **55**, 4067 (2007).
[36] M. L. Falk and J. S. Langer, Annu. Rev. Condens. Matter Phys. **2**, 353 (2011).
[37] H. L. Peng, M. Z. Li, and W. H. Wang, Phys. Rev. Lett. **106**, 135503 (2011).
[38] D. Rodney and C. Schuh, Phys. Rev. Lett. **102**, 235503 (2009).
[39] H. B. Yu, X. Shen, Z. Wang, L. Gu, W. H. Wang, and H. Y. Bai, Phys. Rev. Lett. **108**, 015504 (2012).
[40] H. B. Yu, W. H. Wang, H. Y. Bai, Y. Wu, and M. W. Chen, Phys. Rev. B **81**, 220201(R) (2010).
[41] L. Z. Zhao, R. J. Xue, Z. G. Zhu, K. L. Ngai, W. H. Wang, and H. Y. Bai, J. Chem. Phys. **144**, 204507 (2016).
[42] Q. Wang, S. T. Zhang, Y. Yang, Y. D. Dong, C. T. Liu, and J. Lu, Nat. Commun. **6**, 7876 (2015).
[43] Q. Wang, J. J. Liu, Y. F. Ye, T. T. Liu, S. Wang, C. T. Liu, J. Lu, and Y. Yang, Mater. Today **20**, 293 (2017).
[44] U. Buchenau, Y. M. Galperin, V. L. Gurevich, and H. R. Schober, Phys. Rev. B **43**, 5039 (1991).
[45] J. Bünz, T. Brink, K. Tsuchiya, F. Meng, G. Wilde, and K. Albe, Phys. Rev. Lett. **112**, 135501 (2014).
[46] T. S. Grigera, V. Martín-Mayor, G. Parisi, and P. Verrocchio, Nature (London) **422**, 289 (2003).
[47] V. Gurarie and A. Altland, Phys. Rev. Lett. **94**, 245502 (2005).
[48] M. Kabeya, T. Mori, Y. Fujii, A. Koreeda, B. W. Lee, J.-H. Ko, and S. Kojima, Phys. Rev. B **94**, 224204 (2016).
[49] Y. Li, H. Y. Bai, W. H. Wang, and K. Samwer, Phys. Rev. B **74**, 052201 (2006).
[50] P. Luo, Y. Z. Li, H. Y. Bai, P. Wen, and W. H. Wang, Phys. Rev. Lett. **116**, 175901 (2016).
[51] Y. P. Mitrofanov, M. Peterlechner, S. V. Divinski, and G. Wilde, Phys. Rev. Lett. **112**, 135901 (2014).
[52] W. Schirmacher, G. Diezemann, and C. Ganter, Phys. Rev. Lett. **81**, 136 (1998).
[53] W. Schirmacher, G. Ruocco, and T. Scopigno, Phys. Rev. Lett. **98**, 025501 (2007).
[54] H. Shintani and H. Tanaka, Nat. Mater. **7**, 870 (2008).
[55] A. P. Sokolov, R. Calemczuk, B. Salce, A. Kisliuk, D. Quitmann, and E. Duval, Phys. Rev. Lett. **78**, 2405 (1997).
[56] A. N. Vasiliev, T. N. Voloshok, A. V. Granato, D. M. Joncich, Y. P. Mitrofanov, and V. A. Khonik, Phys. Rev. B **80**, 172102 (2009).
[57] R. C. Zeller and R. O. Pohl, Phys. Rev. B **4**, 2029 (1971).
[58] P. Luo, P. Wen, H. Y. Bai, B. Ruta, and W. H. Wang, Phys. Rev. Lett. **118**, 225901 (2017).
[59] Y. Sun, S. X. Peng, Q. Yang, F. Zhang, M. H. Yang, C. Z. Wang, K. M. Ho, and H. B. Yu, Phys. Rev. Lett. **123**, 105701 (2019).
[60] R. J. Xue, L. Z. Zhao, B. Zhang, H. Y. Bai, W. H. Wang, and M. X. Pan, Appl. Phys. Lett. **107**, 241902 (2015).
[61] S. Plimpton, J. Comput. Phys. **117**, 1 (1995).
[62] W. M. Brown, P. Wang, S. J. Plimpton, and A. N. Tharrington, Comput. Phys. Commun. **182**, 898 (2011).
[63] W. M. Brown, A. Kohlmeyer, S. J. Plimpton, and A. N. Tharrington, Comput. Phys. Commun. **183**, 449 (2012).
[64] W. M. Brown and M. Yamada, Comput. Phys. Commun. **184**, 2785 (2013).
[65] M. I. Mendelev, F. Zhang, Z. Ye, Y. Sun, M. C. Nguyen, S. R. Wilson, C. Z. Wang, and K. Ho, Modell. Simul. Mater. Sci. Eng. **23**, 045013 (2015).
[66] J. Lu, G. Ravichandran, and W. Johnson, Acta Mater. **51**, 3429 (2003).
[67] A. Stukowski, Modell. Simul. Mater. Sci. Eng. **18**, 015012 (2010).